IEEE Access
Multidisciplinary ⋮ Rapid Review ⋮ Open Access Journal

Received December 27, 2020, accepted January 17, 2021, date of publication January 27, 2021, date of current version February 4, 2021.

Digital Object Identifier 10.1109/ACCESS.2021.3054860

Cycle-Life-Aware Optimal Sizing of Grid-Side Battery Energy Storage

YUNFAN ZHANG[1], YIFAN SU[1], ZHAOJIAN WANG[1], (Member, IEEE), FENG LIU[1], (Senior Member, IEEE), AND CHENGHAO LI[2]

[1]State Key Laboratory of Power Systems, Department of Electrical Engineering, Tsinghua University, Beijing 100084, China
[2]State Grid Henan Electric Power Research Institute, Zhengzhou 450052, China

Corresponding author: Feng Liu (lfeng@tsinghua.edu.cn)

This work was supported by the HQ sponsored S&T Project of State Grid Corporation of China 5419-201924207A-0-0-00.

ABSTRACT Grid-side electrochemical battery energy storage systems (BESS) have been increasingly deployed as a fast and flexible solution to promoting renewable energy resources penetration. However, high investment cost and revenue risk greatly restrict its grid-scale applications. As one of the key factors that affect investment cost, the cycle life of battery heavily depends on its charging/discharging actions during the operation, particularly in the presence of uncertain renewable generation. In this context, it is necessary to consider the operation-dependent cycle life of batteries in optimal BESS sizing, which imposes great challenges to the modeling and solving of the planning problems. In this paper, we propose a novel two-level optimal sizing model for grid-scale BESS, considering its operation under uncertainties induced by volatile wind generation. In the lower level, a long-term chronological operation simulation of BESS is processed with an accurate cycle life model of batteries; in the upper level, marginal economic utility analysis and BESS size reforming are conducted to approach the optimal size of BESS. An iterative algorithm is designed to solve the model effectively. The proposed method is verified on a modified IEEE RTS-24 system and a real provincial power grid of China.

INDEX TERMS Battery energy storage, optimal sizing, cycle life, marginal utility analysis.

I. INTRODUCTION

A. BACKGROUND

Recent years have witnessed the proliferation of wind energy, the most popular renewable energy resources. However, the intrinsic stochastic nature of wind power imposes great challenges to power balancing and system secure operation [1]. Distinguished from other technologies, energy storage systems (ESS) can provide a fast and flexible solution to depressing power fluctuations, mitigating load peak-to-valley difference, and flattening load profile, hence facilitating better integration of renewable generation.

Among the current energy storage technologies, electrochemical batteries energy storage systems (BESS) have shown advantages in power density, energy density, dynamic capability, ramp rate and cycle efficiency. With the recent advancements [2], grid-scale battery systems has been drawing constantly increasing attention. However, so far, high-investment cost and revenue risk greatly restrict the deployment of grid-scale batteries [3]. In this context, optimal planning, particularly the sizing of BESS, is key for investment viability. Since BESSs are relatively expensive for their limited life span, battery lifetime assessment is necessary when determining BESS size. Nevertheless, battery cycle life is affected by a set of stress factors, some of which are directly determined by the way a grid-side battery is operated, such as state of charge (SoC) and the depth of discharge (DoD). Thus the cycle life of BESS cannot be determined ex-ante and is operation-dependent. Furthermore, the volatility of wind generation brings further challenges to the prediction of battery lifetime over the BESS project planning horizon. In this paper, we propose a novel sizing model to incorporate precise non-linear BESS lifetime assessment during the planning horizon and develop a two-level iterative algorithm to solve this model effectively.

The associate editor coordinating the review of this manuscript and approving it for publication was Behnam Mohammadi-Ivatloo.

B. LITERATURE REVIEW

To cope with uncertainties induced by volatile renewable generation, optimal BESS planning under uncertainties has been addressed in the literature of joint expansion

planning of distributed generation and distribution networks by scenario-based stochastic programming (SBSP) [4]–[6], chance-constrained stochastic programming (CCSP) [7], robust optimization [8], and distributionally robust optimization [9], where the uncertain demand and renewable generation is captured by a number of discrete representative scenarios, a specific probability distribution, a continuous set of all possible scenarios and an ambiguity set of probability distributions, respectively.

In [4], a mixed binary integer linear programming model is proposed for the optimal BESS allocation for power system integrated with uncertain wind power generation. Benders decomposition is applied to reduce the computational burden resulting from the scenario tree of the wind power output and the involving nonanticipative constraints. References [5], [6] propose a nonlinear scenario-based stochastic programming framework for the joint planning of distribution network and energy storage, considering the impact of BESS and price-dependent demand response programs. The associated scenario-based deterministic equivalence is formulated into a mixed-integer linear program through linearization techniques. Reference [7] considers the integrated planning of electric power generation, natural gas network and storage. A two-stage iterative solution algorithm is provided to solve the chance-constrained mixed integer nonlinear programming problem. In [8] and [9], robust optimization models are applied for BESS planning in transmission networks. The existence of a feasible solution is warranted for any load and renewable energy scenario or distribution in a pre-specified uncertainty set.

The planning results of both robust optimization and stochastic programming rely strongly on the model deployed for the uncertain parameters. Robust optimization based planning has to construct a proper uncertainty set, striking a balance between robustness and economic efficiency. As for the stochastic programming based methods, the selection of probabilistic scenarios is nontrivial [10], with there being a trade-off between computational complexity and representativeness of the scenario set. To get around this, techniques for scenario reduction and decomposition, Monte Carlo simulation, and heuristic algorithms are applied to make the stochastic programming model computationally tractable. But for practically large systems, computational burden remains a challenge.

Regarding battery cycle life, Peukert's law [11] captures the non-linearity relationship between cycle life and DoD of battery, and has been widely used in battery storage involved system designs [3], [12]–[14]. Reference [3] offers mathematical models of battery lifetime assessment by applying Peukert's Law and provides co-optimization bidding strategies balancing battery degradation and profitability in power market. In [12] and [13], energy management and economic scheduling of micro-grid with BESS are presented, respectively, with the consideration of battery lifetime. In [14], a droop control based cycling strategy of BESS is proposed to reduce battery degradation costs. The aforementioned works are built on BESS with a given configuration, i.e., a fixed energy capacity and power rating, and focus on the battery system operation strategies.

It is necessary to equally apply models accounting for battery cycle life and consider the effectiveness of service lifetime when planning decisions are made, so that the battery can be planned and operated more economically [15]. However, due to the intrinsic high nonlinearity of Peukert's law and the discrete logical judgments in the rainflow counting algorithm [16], it is difficult to obtain an analytical expression for the cycle life assessment model and embed it into the planning optimization problem. To this end, several simplified models are adopted [15], [17], [18]. Reference [17] considers sizing and allocation of mobile energy storage for multi-services, where a fixed given project life in years is assumed and linear lifetime constraints are imposed on the battery charge exchanged with the grid. In [15] where co-optimization of active distribution network with energy storage is addressed, piecewise linearized battery lifetime model based on weighted throughput method is utilized to formulate lifetime constraints for Lead-acid battery. In [18], a linear empirical approach based on the cycling ampere-hour that the battery undergoes is adopted to estimate the battery cycle life. Then the cost of energy storage is annualized by the yearly expected life, and a gradient-based searching algorithm is applied to determine the optimal sizing of energy storage for coping with wind power fluctuations. Reference [19] involves an accurate non-linear cycle life model for both first and second life segment of battery. A differential evolutionary algorithm is used to solve the mixed-inter non-linear programming problem, thus a tradeoff between maximizing the profitability of energy storage with multiple functionalities and extending its lifetime duration is achieved.

To conclude, most existing works assume a fixed service life of BESS, or a flat capacity degradation rate, or a simplified cycle life model where battery cycle life is expressed in terms of the charge-discharge power. However, estimation of battery lifetime could be inaccurate and consequently place the viability of BESS under question. To cope with the nonlinearity and discrete logical judgments invoked by Peukert's law and rainflow counting algorithm in sizing problem, heuristic optimization techniques become candidate solutions. Moreover, due to the difference in time scales of long-term planning and short-term operation of the system, dependence of battery cycle life on its operation strategies imposes heavy computational burden on the planning decisions, especially when available wind generation uncertainties exist over the planning horizon.

C. CONTRIBUTION AND ORGANIZATION

1) CONTRIBUTION

To the best of our knowledge, consideration for dependence of BESS lifetime on the operation under uncertainties over the planning horizon has not been included in the existing

literature on grid-side BESS sizing. In this paper, we propose a novel optimal BESS sizing model with accurate cycle life assessment under wind generation uncertainties, and an effective algorithm to solve it. Specifically, we consider optimal sizing of both energy capacity and power rating of BESS. To deal with the lifetime of BESS, we iteratively conduct chronological simulations throughout the life-cycle of BESS and implement size reforming on the energy capacity and power rating. The main contributions of this paper are as follows:

(1) **Modeling**. We propose a two-level optimal BESS sizing model to bridge the yearly planning and hourly operation of BESS, as shown in Fig.1. The upper-level problem is to decide the optimal power and energy capacity of the BESS with a given lifespan of BESS. The lower-level is to simulate the yearly chronological operation of the power system, including hourly BESS regulation under multiple scenarios of renewable generation. Compared with existing works [4]–[9], the proposed model does not rely on specific modeling deployed for uncertain wind generations and accommodates for wide-ranging applications. Compared with existing works [15], [17], [18], the proposed model evaluates cycle-life degradation more accurately since a precise Peukert's Law based cycle life model is utilized for battery lifetime estimation.

(2) **Solution Approach**. We propose an iterative size reforming procedure to coordinate the yearly planning and hourly operation of BESS. Specifically, we evaluate the cycle life of BESS after each-round of hourly chronological operation simulation, and then correct the cycle life of BESS. Afterward, with the corrected cycle life, marginal utility analysis on power and energy capacity of BESS is conducted based on dual shadow prices. It follows a size reforming of BESS to enhance economic efficiency and improve the planning decision. The proposed solution approach can achieve a satisfactory balance between the accuracy of the results and the computing time as demonstrated in the numerical tests using the data of IEEE system and a real provincial power grid of China.

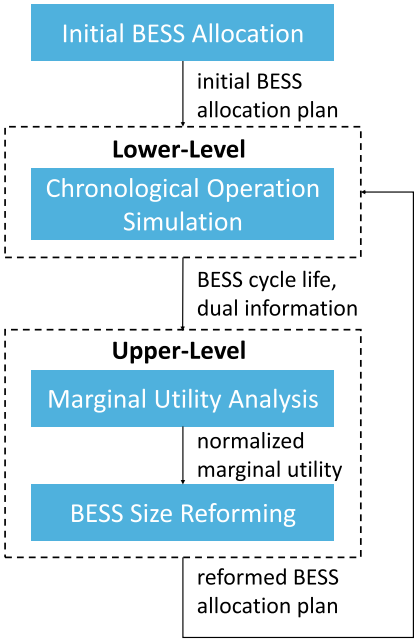

FIGURE 1. Holistic structure of the model.

2) ORGANIZATION

The rest of the paper is organized as follows. The optimal sizing model of grid-side BESS is stated in Section II. Section III introduces the chronological operation simulation on the BESS-integrated power system, where an accurate cycle life model of energy storage battery is considered. Section IV presents marginal utility analysis on the BESS allocation plan and conducts size reforming. Case studies on IEEE system and real-scale provincial power grid are introduced in Section V. Finally, Section VI concludes the paper.

II. OPTIMAL SIZING MODEL OF GRID-SIDE BESS

In this paper, grid-side BESS is allocated to mitigate wind power fluctuations and reduce wind power spillage. Grid-side investors are to determine the optimal BESS sizing (i.e. the energy capacity and power rating of BESS) with the goal of economical optimality of the entire grid system. Considering the high uncertainty and volatility of wind power, a scenario-based stochastic programming method is employed to derive an initial BESS allocation strategy.

A. OBJECTIVE FUNCTION

The objective function of the optimization problem is:

$$\min_{P_{\mathrm{BES}},E_{\mathrm{BES}}} \left(\pi^{\mathrm{BES}} + \pi^{\mathrm{wc}} + \pi^{\mathrm{ls}} + \pi^{\mathrm{g}}\right) \tag{1}$$

where the decision variables, P_{BES} and E_{BES}, denote the power rating and energy capacity of BESS, respectively. The objective in (1) consists of investment costs of BESS π^{BES}, production costs of conventional generators π^{g}, penalty of curtailments on wind power π^{wc}, as well as the penalty of load shedding π^{ls}. The aforementioned cost items will be explained as follows:

1) INVESTMENT COST OF BESS

π^{BES} denotes the total investment cost of BESS that being divided into each year, with a specific formation of

$$\pi^{\mathrm{BES}} = AF\left(C^{\mathrm{ep}}P_{\mathrm{BES}} + C^{\mathrm{ee}}E_{\mathrm{BES}}\right) \tag{2}$$

$$AF = \frac{I(1+I)^{Y^{\mathrm{ep}}}}{(1+I)^{Y^{\mathrm{ep}}}-1}. \tag{3}$$

In (2), C^{ep} and C^{ee} are the unit investment cost of the power rating and energy capacity of BESS, respectively. The BESS total fixed investment cost $(C^{\mathrm{ep}}P_{\mathrm{BES}}+C^{\mathrm{ee}}E_{\mathrm{BES}})$ is converted to an annual value by multiplying the annuity factor (AF) AF. This factor is defined in (3) where I denotes the discount rate

of grid-side BESS equipment, and Y^{ep} denotes the anticipated battery shelf life in years.

2) COST OF WIND CURTAILMENT

To promote renewable energy accommodation, penalties on the curtailment of wind are considered. π^{wc} denotes the annual cost of wind curtailment, with a specific formation of

$$\pi^{\mathrm{wc}} = 365 \sum_{s\in\mathcal{S}} \sum_{t\in\mathcal{T}} \sum_{i\in\mathcal{W}} \omega_s C_i^{\mathrm{wc}} \left(p_{s,t,i}^{\mathrm{wg,max}} - p_{s,t,i}^{\mathrm{wg}}\right) \quad (4)$$

where C_i^{wc} is the penalty coefficient for unit curtailed wind power of wind farm i. $p_{s,t,i}^{\mathrm{wg,max}}$ and $p_{s,t,i}^{\mathrm{wg}}$ denote the hourly available wind power and the hourly consumed wind power of wind farm i at time slot t in scenario s. ω_s is the discrete probability of scenario s. $\mathcal{S}$ represents the set of selected scenarios, $\mathcal{T}$ denotes the set of time slots in a scenario, and $\mathcal{W}$ denotes the set of wind farms.

3) COST OF LOAD SHEDDING

π^{ls} denotes the annual cost of load shedding, with a specific formation of

$$\pi^{\mathrm{ls}} = 365 \sum_{s\in\mathcal{S}} \sum_{t\in\mathcal{T}} \sum_{i\in\mathcal{N}} \omega_s C_i^{\mathrm{ls}} \left(p_{s,t,i}^{\mathrm{le}} - p_{s,t,i}^{\mathrm{l}}\right) \quad (5)$$

where C_i^{ls} denotes the loss of unit load shedding at bus i, $p_{s,t,i}^{\mathrm{le}}$ and $p_{s,t,i}^{\mathrm{l}}$ denote the active power demand and the active power consumption of bus i at time slot t in scenario s, respectively. $\mathcal{N}$ denotes the set of buses in the grid.

4) COST OF CONVENTIONAL GENERATORS

π^{g} denotes the annual generation cost of conventional generators, with a specific formation of

$$\pi^{\mathrm{g}} = 365 \sum_{s\in\mathcal{S}} \sum_{t\in\mathcal{T}} \sum_{i\in\mathcal{G}} \omega_s \left(C_i^2 (p_{s,t,i}^{\mathrm{g}})^2 + C_i^1 p_{s,t,i}^{\mathrm{g}} + C_i^0\right) \quad (6)$$

where $p_{s,t,i}^{\mathrm{g}}$ denotes the active power output of conventional generator i at time slot t under scenario s. $\mathcal{G}$ is the set of all conventional generators. C_i^0, C_i^1, C_i^2 are the cost coefficients of conventional generator i.

B. RESTRAINT CONDITIONS

This model is based on a direct current (DC) power flow [20] and leaves out the reactive power of BESS and network. This simplification is adopted in many existing studies [3]–[9], [15], [18], [19], since BESS's support on real power balance is the main focus. All constraints are listed as follows.

1) RESTRAINT CONDITIONS OF CONVENTIONAL GENERATORS

The active output of conventional generators should fulfill the following operation conditions:

$$p_i^{\mathrm{g,min}} \le p_{s,t,i}^{\mathrm{g}} \le p_i^{\mathrm{g,max}}, \quad \forall s \in \mathcal{S}, t \in \mathcal{T},\ i \in \mathcal{G} \quad (7)$$

$$|p_{s,t,i}^{\mathrm{g}} - p_{s,t-1,i}^{\mathrm{g}}| \le p_i^{\mathrm{gr}}, \quad \forall s \in \mathcal{S},\ t \in \mathcal{T}, i \in \mathcal{G} \quad (8)$$

where $p_i^{\mathrm{g,min}}$ and $p_i^{\mathrm{g,max}}$ represent the minimal and maximal active output of conventional generator i, respectively; and p_i^{gr} denotes the ramping rate of conventional generator i.

2) RESTRAINT CONDITIONS OF WIND OUTPUT

The wind power consumption should be limited by its available maximal wind output:

$$0 \le p_{s,t,i}^{\mathrm{wg}} \le p_{s,t,i}^{\mathrm{wg,max}}, \quad \forall s \in \mathcal{S},\ t \in \mathcal{T},\ i \in \mathcal{W}. \quad (9)$$

3) RESTRAINT CONDITIONS OF LOAD SHEDDING

The actual active power consumption of bus i at time slot t under scenario s should be limited by its active power demand:

$$0 \le p_{s,t,i}^{\mathrm{l}} \le p_{s,t,i}^{\mathrm{le}}, \quad \forall s \in \mathcal{S},\ t \in \mathcal{T},\ i \in \mathcal{N}. \quad (10)$$

4) RESTRAINT CONDITIONS OF BATTERY ENERGY STORAGE

The charging and discharging of BESS should fulfill the following conditions:

$$0 \le p_{s,t}^{\mathrm{ch}} \le P_{\mathrm{BES}}, \quad \forall s \in \mathcal{S},\ t \in \mathcal{T} \quad (11)$$

$$0 \le p_{s,t}^{\mathrm{dc}} \le P_{\mathrm{BES}}, \quad \forall s \in \mathcal{S},\ t \in \mathcal{T} \quad (12)$$

$$p_{s,t}^{\mathrm{ch}} \cdot p_{s,t}^{\mathrm{dc}} = 0, \quad \forall s \in \mathcal{S},\ t \in \mathcal{T} \quad (13)$$

$$\underline{\mu} \cdot E_{\mathrm{BES}} \le E_{s,t} \le \overline{\mu} \cdot E_{\mathrm{BES}}, \quad \forall s \in \mathcal{S},\ t \in \mathcal{T} \quad (14)$$

$$E_{s,t} = E_{s,t-1} + \eta^{\mathrm{ch}} \cdot p_{s,t}^{\mathrm{ch}} - \frac{p_{s,t}^{\mathrm{dc}}}{\eta^{\mathrm{dc}}}, \quad \forall s \in \mathcal{S},\ t \in \mathcal{T} \quad (15)$$

$$E_0 = E_{|\mathcal{T}|} \quad (16)$$

where $p_{s,t}^{\mathrm{ch}}$, $p_{s,t}^{\mathrm{dc}}$ and $E_{s,t}$ are the charge power, discharge power and the energy of BESS at time slot t in scenario s, respectively. Constraints (11)-(12) imply that the charging and discharging power of BESS are limited by its power rating. Constraint (13) is the complementarity constraint of BESS device. η^{ch} and η^{dc} are the charging and discharging efficiencies of BESS. $\overline{\mu}$ and $\underline{\mu}$ are the upper and lower limits of the SoC of BESS, respectively. Constraint (14) is the restraint condition of energy storage capacity. Constraints (15) and (16) guarantee the energy balance of BESS where $|\mathcal{T}|$ denotes the total number of time slots.

5) RESTRAINT CONDITIONS OF POWER NETWORK

Power balance constraint (17) ensures the sum of all types of generation is equal to total power consumption at each time interval.

$$\sum_{i\in\mathcal{G}} p_{s,t,i}^{\mathrm{g}} + \sum_{i\in\mathcal{W}} p_{s,t,i}^{\mathrm{wg}} + p_{s,t}^{\mathrm{dc}} = p_{s,t}^{\mathrm{ch}} + \sum_{i\in\mathcal{N}} p_{s,t,i}^{\mathrm{l}}, \quad \forall s \in \mathcal{S},\ t \in \mathcal{T} \quad (17)$$

Let $p_{s,t,l}^{\mathrm{line}}$ denote the power flow on transmission line l at time t in scenario s. For any scenario $s \in \mathcal{S}$, time $t \in \mathcal{T}$ and any transmission line $l \in \mathcal{L}$:

$$p_{s,t,l}^{\mathrm{line}} = \sum_{i\in\mathcal{G}} \mathrm{GSF}_{l,i}^{\mathrm{g}} \cdot p_{s,t,i}^{\mathrm{g}} + \sum_{i\in\mathcal{W}} \mathrm{GSF}_{l,i}^{\mathrm{wg}} \cdot p_{s,t,i}^{\mathrm{wg}}$$

$$-\sum_{i\in\mathcal{N}} \mathrm{GSF}_{l,i}\cdot p^{\mathrm{l}}_{s,t,i} + \mathrm{GSF}^{\mathrm{BES}}_{l}\cdot\left(p^{\mathrm{dc}}_{s,t}-p^{\mathrm{ch}}_{s,t}\right) \quad (18)$$

where $\mathrm{GSF}_{l,i}$ is the generation shift factor (GSF) to line l from bus i; $\mathrm{GSF}^{\mathrm{g}}_{l,i}$ the GSF to line l from generator i; $\mathrm{GSF}^{\mathrm{wg}}_{l,i}$ the GSF to line l from wind farm i; $\mathrm{GSF}^{\mathrm{BES}}_{l}$ the GSF to line l from the BESS; $\mathcal{L}$ is the set of transmission lines in the power grid. Constraint (19) enforces the bidirectional power flow limits of the transmission lines.

$$-p^{\mathrm{line,max}}_{l} \le p^{\mathrm{line}}_{s,t,l} \le p^{\mathrm{line,max}}_{l},\ \forall s\in\mathcal{S},\ t\in\mathcal{T}, l\in\mathcal{L}. \quad (19)$$

C. FINDING INITIAL BESS ALLOCATION STRATEGY

To determine an initial allocation strategy of grid-side BESS considering the uncertainty of wind output, first, we select eight typical scenarios consisting of four daily wind curves with the most significant reverse peak regulation characteristics, of spring, summer, autumn and winter, respectively, and two daily load curves of working day and non-working day, respectively. Then a BESS-concerned SBSP is established as (20), where the typical scenes are intuitively assigned equal probabilities.

$$\begin{aligned}&\min_{P_{\mathrm{BES}},E_{\mathrm{BES}}} \left(\pi^{\mathrm{BES}}+\pi^{\mathrm{wc}}+\pi^{\mathrm{ls}}+\pi^{\mathrm{g}}\right)\\ &\text{subject to (7)-(19)}\end{aligned} \quad (20)$$

Note that the storage operational cost is neglected in (20) as the grid-side BESS is owned by the power grid company itself. The bi-linear constraint (13) makes the problem (20) strongly non-convex and difficult to solve. Usually, the complementarity constraint (13) can be precisely linearized by introducing auxiliary binary variables [21]. Moreover, the (epigraph of) quadratic generation cost function π^{g} can be piecewise linearized. Thus (20) is converted into a mixed integer linear programming (MILP). Then the optimal solution to problem (20), $(P^0_{\mathrm{BES}}, E^0_{\mathrm{BES}})$, is set as the initial BESS allocation strategy.

III. CHRONOLOGICAL OPERATION SIMULATION OF THE BESS-INTEGRATED POWER SYSTEM

By solving the multi-scenario stochastic programming (20), an initial grid-side BESS allocation strategy $(P^0_{\mathrm{BES}}, E^0_{\mathrm{BES}})$ is obtained. However, this configuration scheme is based on a limited number of typical scenes, not fully considering the impact of wind uncertainties. Moreover, this planning assumes that the BESS has a fixed lifetime Y^{ep}, which may be not valid if the BESS has more or less frequent cycling than expected. As a matter of fact, the real lifetime of battery is sensitive to operation. In this regard, we run a life-cycle chronological operation simulation (COS) on the given configuration scheme to estimate the realistic service life of BESS, and then adjust the allocation plan through marginal benefit analysis that will be introduced in Section IV. This design is economically optimal while addressing the uncertainties of wind power and the unique degradation characteristics of BESS.

A. CYCLE-LIFE MODEL OF BESS

Electrochemical batteries have limited cycle life because of the fading of active materials caused by the charging and discharging cycles. In this paper, we focus on lithium-ion batteries, for which the DoD is the most important operational factor in battery degradation and cycle life assessment. The lithium-ion BESS can perform a certain number of cycles at a specific DoD [3]:

$$N^{\mathrm{fail}}_{d} = N^{\mathrm{fail}}_{100}\cdot d^{-\mathrm{k_P}} \quad (21)$$

where N^{fail}_{d} and N^{fail}_{100} are the maximum number of charge-discharge cycles at a specific DoD of d and a DoD of 100% before the battery's failure, respectively. $\mathrm{k_P}$ and N^{fail}_{100} are positive inherent parameters that can be provided by the battery manufacturer. By keeping the loss of cycle life a constant, the equivalent 100%-DoD cycle number n^{eq}_{100} of n_d cycles at DoD of d is derived as:

$$n^{\mathrm{eq}}_{100} = n_d\cdot d^{\mathrm{k_P}}, \quad (22)$$

implying that a deeper DoD, a smaller $\mathrm{k_P}$ or more frequent cycles (i.e., a larger n_d) gives rise to a shorter service life of the battery.

A full cycle consists of one charging half cycle and one discharging half cycle with the same DoD. In reality, however, two contiguous charge/discharge sessions might be asymmetric. In this regard, the rainflow counting method [16] is applied to an SoC profile to identify cycles. Consider a daily SoC profile SoC^{day}, the rainflow algorithm outputs all the cycle depth as:

$$\left(d^{\mathrm{half}}, d^{\mathrm{full}}\right) = \mathrm{Rainflow}\left(\mathrm{SoC}^{day}\right) \quad (23)$$

where d^{half} is the vector of half cycles and d^{full} is the vector of full cycles. For the specific steps of rainflow algorithm, see [16]. Thus a battery's daily equivalent 100%-DoD cycle number is derived:

$$n^{\mathrm{eq},day}_{100} = \sum\nolimits_j 0.5\left(d^{\mathrm{half}}_j\right)^{\mathrm{k_P}} + \sum\nolimits_j \left(d^{\mathrm{full}}_j\right)^{\mathrm{k_P}}. \quad (24)$$

Then the realistic yearly service life of BESS is

$$Y^{\mathrm{rl}} = \frac{N^{\mathrm{fail}}_{100}}{\sum_{day=1}^{365} n^{\mathrm{eq},day}_{100}} \quad (25)$$

which may be different from the expected one Y^{ep}. This discordance may affect the economical optimality of BESS allocation strategy. Next, we will show how realistic service life is obtained through all-year chronological operation simulation.

B. CHRONOLOGICAL OPERATION SIMULATION

1) STEP 1: DATA PREPARATION

First, we prepare data for the long-term BESS-concerned chronological operation simulation: the wind output profiles, load forecasts, parameters of conventional generators and states of critical tie-lines are needed. The annual chronological wind output profiles can be obtained by utilizing historical

measured data, or generated according to meteorological data and the output characteristics of wind turbine generators. Note that possible future expansion on system load during the simulated period can be taken into account.

2) STEP 2: DAILY OPERATION MODELING AND EVOLVING

Given the BESS allocation plan, year around operations are simulated by consecutively running daily simulations to analyze the interactions between the renewable generations and grid-side BESS during the whole-life-cycle of BESS. To this end, a daily COS model is formulated to find the optimal hourly operation of BESS which is characterized by the daily SoC profile SoC^{day}, and that of the conventional generators. Note that simulations on days can be carried out in parallel to accelerate the annual COS.

By reducing (20) into one scenario (i.e., one specific day) and substituting P_{BES} and E_{BES} by the given allocation scheme $\left(P^k_{\mathrm{BES}}, E^k_{\mathrm{BES}}\right)$ (when $k = 0$ it denotes the initial allocation plan), a BESS-integrated DC optimal power flow problem is formulated as the daily operation model of COS. Note that in the daily operation model, the complementarity constraint of BESS, equality (13), is relaxed to simplify the problem into a linear program to accelerate the computation. Though this may give rise to the situation that charging and discharging occur simultaneously, its influence on BESS's lifetime is quantified by recording the daily SoC profile.

Moreover, the duality of the linear BESS-integrated DC optimal power flow problem is solved, for the dual variables of constraint (11), (12) and (14) are needed to calculate the marginal revenue (MR) of the BESS, as further explained in the Subsection IV. Notations are taken as follows:

$$\underline{\mu} \cdot E^k_{\mathrm{BES}} \le E^{day}_t \le \overline{\mu} \cdot E^k_{\mathrm{BES}} \quad (\text{dual: } \underline{\lambda}^{day}_t, \overline{\lambda}^{day}_t) \tag{26}$$

$$p^{\mathrm{ch},day}_t \le P^k_{\mathrm{BES}} \quad (\text{dual: } \phi^{\mathrm{ch},day}_t) \tag{27}$$

$$p^{\mathrm{dc},day}_t \le P^k_{\mathrm{BES}} \quad (\text{dual: } \phi^{\mathrm{dc},day}_t) \tag{28}$$

3) STEP 3: RESULT OUTPUT

After the modeling and solving step, results from all parallel daily processes are combined as an annual outturn. First, a realistic service life of BESS in years, Y^{rl}, is obtained through (23)-(25). Moreover, values of dual multipliers $\underline{\lambda}$, $\overline{\lambda}$, ϕ^{ch} and ϕ^{dc} are recorded.

IV. MARGINAL UTILITY ANALYSIS AND SIZE REFORMING OF BESS

In this section, given the results from the chronological operation simulation, the optimality of the BESS allocation is evaluated from the perspective of marginal utility (MU), which is defined as the difference between the MR and the marginal cost (MC). In economic theory, MU analysis is an effective tool to help companies determine the optimal yield of goods. A firm should expand production until the point where MC is equal to MR. Motivated by this, the relationship between the MR and MC of the power/energy capacity of BESS helps to find the optimal sizing that maximizes system utility, especially when the MR and MC are evaluated under the realistic cycle life of BESS.

A. MARGINAL REVENUE OF BESS

An annualized marginal grid-side benefit provided by the BESS is calculated based on the annual COS results, as in (29) and (30).

$$MR^{\mathrm{P}}_{\mathrm{BES}} = \sum\nolimits_{day=1}^{365} \sum\nolimits_{t\in\mathcal{T}} \left(\phi^{\mathrm{ch},day}_t + \phi^{\mathrm{dc},day}_t\right) \tag{29}$$

$$MR^{\mathrm{E}}_{\mathrm{BES}} = \sum\nolimits_{day=1}^{365} \sum\nolimits_{t\in\mathcal{T}} \left(\overline{\mu} \cdot \overline{\lambda}^{day}_t - \underline{\mu} \cdot \underline{\lambda}^{day}_t\right) \tag{30}$$

For the BESS with current sizing which is $\left(P^k_{\mathrm{BES}}, E^k_{\mathrm{BES}}\right)$, $MR^{\mathrm{P}}_{\mathrm{BES}}$ is the annualized MR of its power capacity and $MR^{\mathrm{E}}_{\mathrm{BES}}$ is the annualized MR of its energy capacity. Namely, additional per unit of capacity of power (energy) can reduce the yearly costs of system by $MR^{\mathrm{P}}_{\mathrm{BES}}$ ($MR^{\mathrm{E}}_{\mathrm{BES}}$) when additional BESS investment cost is not considered. Note that this marginal contribution of BESS to power system is evaluated fully considering the fluctuations of wind power throughout the year.

B. MARGINAL COST OF BESS

The MC of BESS is calculated based on its life span as in (31) and (32)

$$MC^{P}_{\mathrm{BES}}(Y) = \frac{I(1+I)^Y}{(1+I)^Y - 1} C^{\mathrm{ep}} \tag{31}$$

$$MC^{E}_{\mathrm{BES}}(Y) = \frac{I(1+I)^Y}{(1+I)^Y - 1} C^{\mathrm{ee}} \tag{32}$$

where C^{ep} and C^{ee} are investment cost for per-unit of the capacity of power and energy of BESS, respectively, and are converted into annual values. If Y takes the value of a fixed expected cycle life Y^{ep}, then the capacity of power or energy has a fixed MC. If Y takes the value of a realistic cycle life Y^{rl}, then the MC of BESS configuration can be varying and operation-dependent. Note that only one-time investment cost is considered here. Since the grid-side BESS is controlled by operators, operation costs caused by unmet discharged or charged energy does not exist. Additional operational cost, e.g. damage to the state of health of BESS caused by over-charge/-discharge, can be indirectly considered through the operation-dependent variable life span Y^{rl}.

C. SIZE REFORMING OF BESS

The normalized MU of the capacity of power and energy of BESS can be calculated by (33) and (34), respectively. If the corresponding MU is greater than zero, additional capacity allocation to the current scheme is economically beneficial to the system, till the point MU decreasing to zero. Otherwise, a reduction on the current configuration of BESS is better, till the point MU increasing to 0.

$$MU^{\mathrm{P}}_{\mathrm{BES}} = \frac{MR^{\mathrm{P}}_{\mathrm{BES}} - MC^{\mathrm{P}}_{\mathrm{BES}}(Y^{\mathrm{rl}})}{\max\left(MR^{\mathrm{P}}_{\mathrm{BES}}, MC^{\mathrm{P}}_{\mathrm{BES}}(Y^{\mathrm{rl}})\right)} \tag{33}$$

$$MU^{\mathrm{E}}_{\mathrm{BES}} = \frac{MR^{\mathrm{E}}_{\mathrm{BES}} - MC^{\mathrm{E}}_{\mathrm{BES}}(Y^{\mathrm{rl}})}{\max\left(MR^{\mathrm{E}}_{\mathrm{BES}}, MC^{\mathrm{E}}_{\mathrm{BES}}(Y^{\mathrm{rl}})\right)} \tag{34}$$

Therefore, if $|MU^{\mathrm{P}}_{\mathrm{BES}}|$ and $|MU^{\mathrm{E}}_{\mathrm{BES}}|$ are both less than a pre-set precision $\epsilon > 0$, we regard the current allocation plan $\left(P^{k}_{\mathrm{BES}}, E^{k}_{\mathrm{BES}}\right)$ as optimal. Otherwise, we do size reforming on the current scheme $\left(P^{k}_{\mathrm{BES}}, E^{k}_{\mathrm{BES}}\right)$ as in (35) and (36).

$$P^{k+1}_{\mathrm{BES}} = P^{k}_{\mathrm{BES}} \cdot \left(1 + \alpha \cdot MU^{\mathrm{P}}_{\mathrm{BES}}\right) \tag{35}$$

$$E^{k+1}_{\mathrm{BES}} = E^{k}_{\mathrm{BES}} \cdot \left(1 + \alpha \cdot MU^{\mathrm{E}}_{\mathrm{BES}}\right) \tag{36}$$

k here denotes the iteration round of size reforming and $\alpha > 0$ is the step size which can be a fixed value or vary with the step k. The adjusted configuration plan is denoted by $\left(P^{k+1}_{\mathrm{BES}}, E^{k+1}_{\mathrm{BES}}\right)$. Then annual COS on the $\left(P^{k+1}_{\mathrm{BES}}, E^{k+1}_{\mathrm{BES}}\right)$-integrated power system is needed, for further marginal utility analysis on this configuration.

The block diagram for the proposed optimal BESS sizing method based on simulation-based marginal utility analysis is illustrated in Fig.2.

V. CASE STUDY

In this section, we test the proposed annual COS and MU analysis based grid-side BESS allocation strategy. Simulations are carried out on a modified IEEE RTS-24 buses system and a provincial system of China, with MATLAB on a laptop with Intel(R) Core(TM) i5-5200U 2.20GHz CPU and 4GB of RAM.

A. SETUP

We do some modifications to the IEEE RTS-24 system:

1) A wind farm with a capacity of 300MW is located at bus 1. The BESS candidate position is also bus 1.
2) The active power load of the system is modified as in Table.1.
3) The power limits of transmission lines (1,2), (1,3) and (1,5) are set as 80MW, 50MW, 80MW, respectively.

TABLE 1. The proportion of each load.

Load	Bus	Proportion	Load	Bus	Proportion
L1	1	1.79%	L10	10	6.98%
L2	2	3.47%	L11	13	9.49%
L3	3	6.45%	L12	14	6.95%
L4	4	2.65%	L13	15	11.35%
L5	5	2.54%	L14	16	3.58%
L6	6	4.87%	L15	18	11.93%
L7	7	4.48%	L16	19	6.48%
L8	8	6.12%	L17	20	4.58%
L9	9	6.27%			

The modified IEEE RTS-24 system is shown in Fig.3. Parameters about line impedance, line capacity and conventional generators can be found in [22]. For cost coefficients of conventional generators, see Matpower CASE24_IEEE_RTS data file [23].

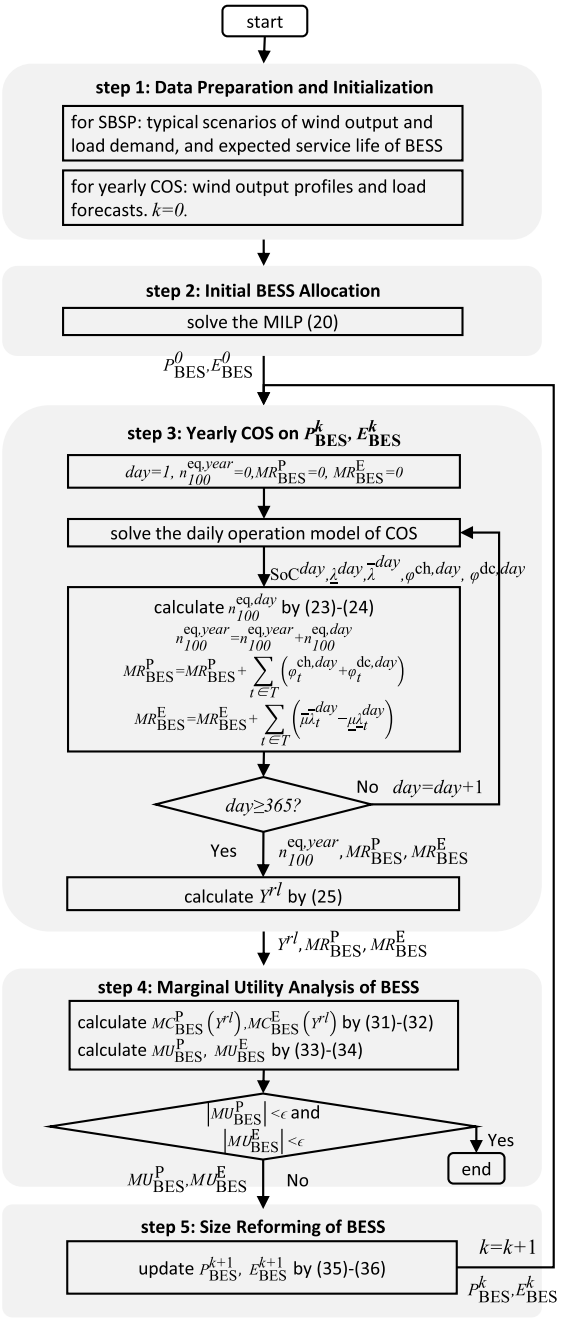

FIGURE 2. The specific steps of optimal BESS sizing based on simulation-based marginal utility analysis.

Limited by the capacity of sent-out gateway as well as the reverse peak regulation characteristics of wind power, the wind farm at bus 1 suffers from wind curtailment. To mitigate wind power fluctuations and reduce wind power spillage, grid owner plans to allocate a battery energy storage system nearby, i.e., at bus 1.

Two typical daily load profiles are considered: working day and non-working day, as shown in Fig.4(a). The peak load of the system on the working day is 3165.6MW, and that of the non-working day is 2648MW. The wind power data

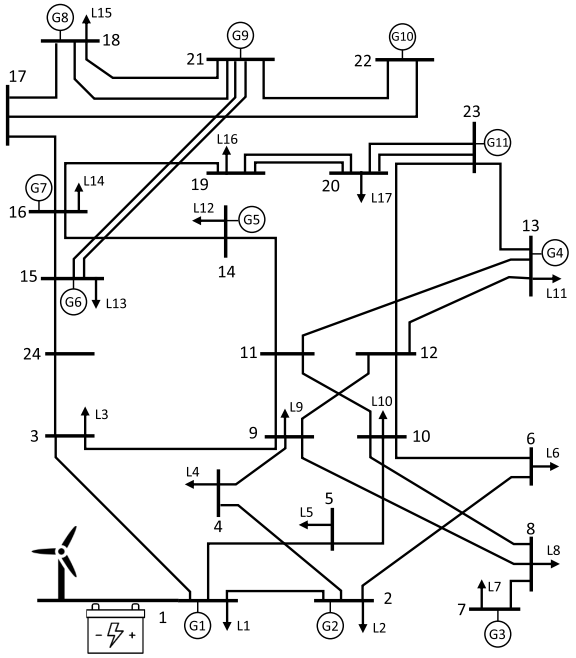

FIGURE 3. Modified IEEE RTS-24 system.

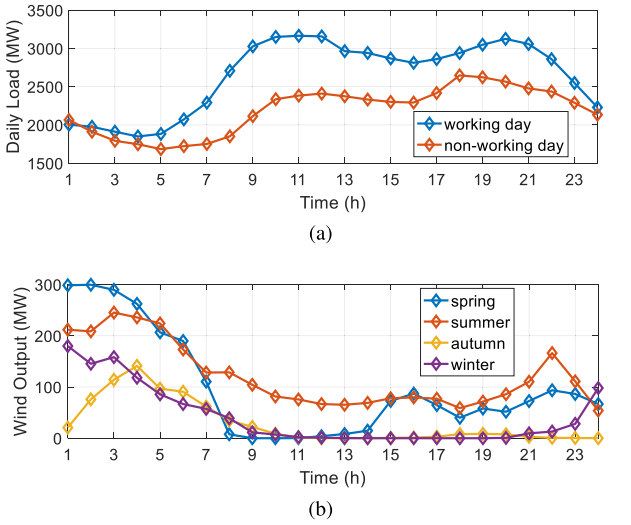

FIGURE 4. (a) Two typical daily total load profiles. (b) Typical wind output curves of four seasons.

come from 2012 NREL position (116.6W°,36.9N°) and we scale it to fit the capacity of 300MW. Fig.4(b) shows four representative daily wind curves with the most significant reverse peak regulation characteristics of spring, summer, autumn and winter, respectively. Wind generation is assumed to have zero marginal cost and is hence free.

The BESS-related parameters are given in Table.2.

TABLE 2. The BESS-related parameters.

Parameter	Value	Parameter	Value
C^{ee}	200,000$/MW.h	I	4.9%
C^{ep}	50,000$/MW	η^{ch}	90%
N_{100}^{fail}	2000	η^{dc}	90%
Y^{ep}	8 year	$\overline{\mu}$	0.9
k_P	1.25	$\underline{\mu}$	0.1

TABLE 3. Cost of modified IEEE RTS-24 system without BESS (uniform annual value, unit: million USD per year).

Typical Scenario	Total Cost	Generation	Wind Curtailment	Load Shedding
Working Day, Spr.	579.43	503.48	65.95	10.00
Working Day, Sum.	539.35	497.16	31.44	10.75
Working Day, Aut.	499.49	499.49	0	0
Working Day, Win.	502.61	501.08	0	0
Non-working Day, Spr.	480.75	406.03	67.97	6.75
Non-working Day, Sum.	443.38	404.60	32.55	6.23
Non-working Day, Aut.	402.29	402.29	0	0
Non-working Day, Win.	405.13	403.62	0	1.51
Average Value	481.55	452.22	24.74	4.60

TABLE 4. Cost of modified IEEE RTS-24 system with initial BESS plan (uniform annual value, unit: million USD per year).

Total Cost	BESS Investment	Generation	Wind Curtailment	Load Shedding
467.87	16.76	447.43	1.75	1.93

B. SIMULATION RESULTS

1) INITIAL BESS ALLOCATION BASED ON SBSP

First, we solve the multi-period DC-OPF model for the cost of the modified IEEE RTS-24 system without grid-side BESS devices under 8 typical scenarios. The cost of system without BESS is shown in Table.3. Wind spillage and curtailment occur in the scene of spring and summer, during midnight. Consequently, the system pays for an annual penalty cost of 24.74 million USD, contributing to 5.14% of the annual total costs.

Then, we solve the scenario-based stochastic programming (20) and obtain an initial BESS configuration: P_{BES}^0 is 97.87MW and E_{BES}^0 is 519.35MW.h. Cost of the modified IEEE RTS-24 system with the BESS allocation of $\left(P_{BES}^0, E_{BES}^0\right)$ is shown in Table.4. With this BESS configuration, the annual comprehensive cost is reduced by 2.84%, from 481.55 million USD to 467.87 million USD. This is because the integration of BESS increases short-term system operation flexibility, permitting greater participation of wind and reducing the generation cost of conventional generators and penalty on wind curtailment. Fig.5 shows the wind consumption curve with and without BESS adjacent to the wind farm, as well as the charge/discharge profiles of the BESS. It can be seen from Fig.5 that when the expected output of a wind farm is large, it is often accompanied by charging of energy storage to reduce wind abandonment. When the

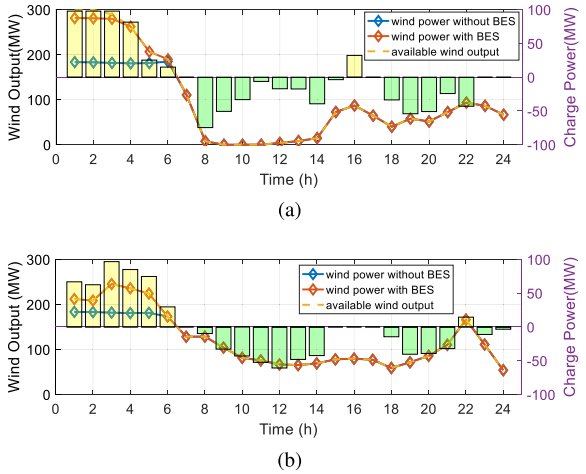

FIGURE 5. Wind power without and with BESS. (a) Working day of Spring. (b) Working day of summer.

expected output of wind farm is small, BESS will release energy to reduce the fluctuation of the joint wind farm.

2) MARGINAL UTILITY ANALYSIS AND SIZE REFORMING

Given the initial BESS allocation plan, we analyze the marginal utility of power rating P^0_{BES} which is 97.87MW and energy capacity E^0_{BES} which is 519.35MW.h, through annual chronological operation simulation. The annual COS and size reforming process is iteratively done to find the configuration that has both zero $MU^{\mathrm{P}}_{\mathrm{BES}}$ and zero $MU^{\mathrm{E}}_{\mathrm{BES}}$. The final configuration result would be optimal concerning wind fluctuations throughout the year and operation-dependent battery cycle life.

Size reforming on power rating and energy capacity are shown in Fig.6 (a) and (b), respectively. Note that results in these two subfigures come from the same iterative process, since E_{BES} and P_{BES} are two configuration parameters coupled in one system and consequently cannot be analyzed separately. After 14 rounds of COS and size reforming, the final BESS configuration plan is as follows: P^{14}_{BES} is 123.27MW, with $MC^{\mathrm{P}}_{\mathrm{BES}}(Y^{\mathrm{rl}})$ being 7762.15\$, $MR^{\mathrm{P}}_{\mathrm{BES}}$ being 7939.32\$, and the normalized marginal utility of power rating $MU^{\mathrm{P}}_{\mathrm{BES}}$ being 2.23% which is smaller than the pre-set tolerance $\epsilon = 5\%$; E^{14}_{BES} is 465.11MW.h, with $MC^{\mathrm{E}}_{\mathrm{BES}}(Y^{\mathrm{rl}})$ being 31048.62\$, $MR^{\mathrm{E}}_{\mathrm{BES}}$ beging 30124.35\$, and the normalized marginal utility of energy capacity being 2.98%. Realistic BESS life derived through an accurate cycle life model is presented in Fig.6(c), indicating that the anticipated service life of BES may deviate from its real life a lot.

Fig.6(a) also shows that the MR of the BESS power rating decreases with increasing power rating configuration. Similarly, Fig.6(b) indicates that the MR of BESS energy capacity increases with decreasing battery capacity. These are coincident with the theoretical result in [24] that the marginal value from storage (without considering investment cost) is decreasing with storage size.

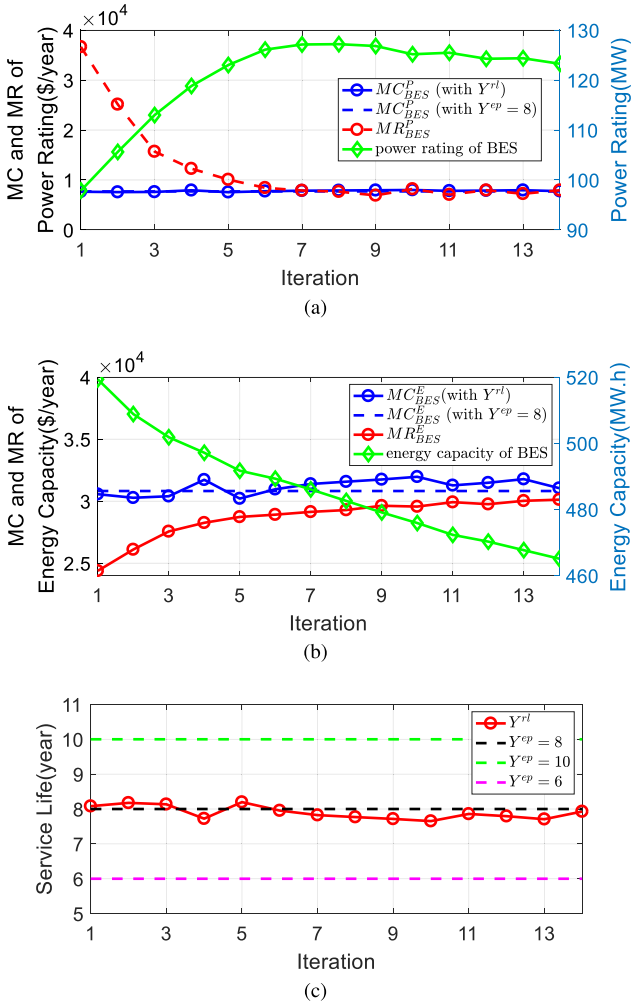

FIGURE 6. (a) Power rating reforming of BESS. (b) Energy capacity reforming of BESS. (c) Realistic and expected life of BESS.

3) VERIFICATION OF OPTIMALITY

Theoretically, the simulation-based marginal utility analysis cannot characterize the sensitivity relationship between all values of continuous decision variables P_{BES}, E_{BES} and the objective function. In this subsection, we verify that the proposed method achieves an error-bounded configuration plan within 14 rounds of annual COS and size reforming iterations. First, we discretize the continuous configuration parameters P_{BES}, E_{BES} into a two-dimensional grid with adaptive pixels. Then we run annual COS on each pixel and map the normalized MU on this grid.

The range of P_{BES} is [97,128]MW and the range of E_{BES} is [425,522]MW.h. In order to alleviate computation burden as well as ensure the accuracy of the contour map, the size of pixels is varying and adaptive to local steepness. The contour map of $MU^{\mathrm{P}}_{\mathrm{BES}}$ is shown in Fig.7(a) and that of $MU^{\mathrm{E}}_{\mathrm{BES}}$ is depicted in Fig.7(b). In addition, the trajectory of size forming is given, showing how the initial configuration is adjusted to the point within pre-set tolerance $\epsilon = 5\%$.

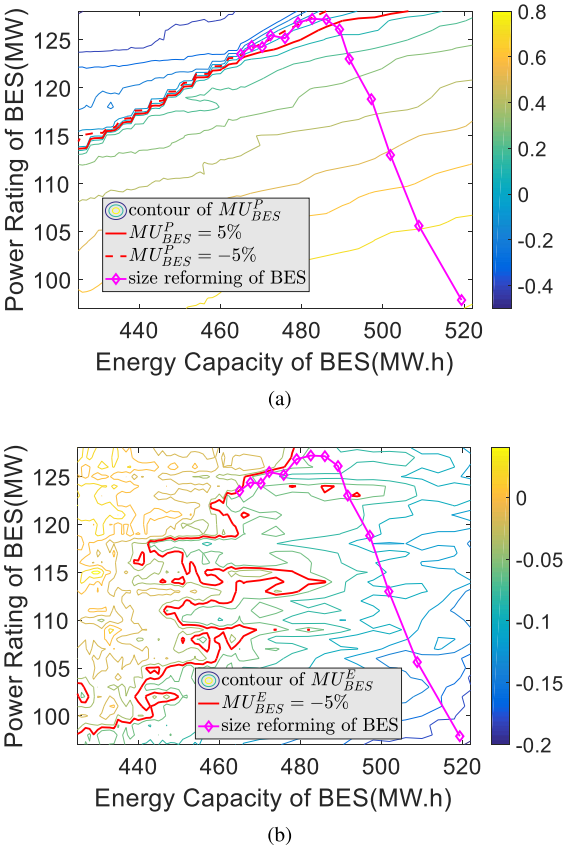

FIGURE 7. (a) Contour map of MU^P_{BES}. (b) Contour map of MU^E_{BES}.

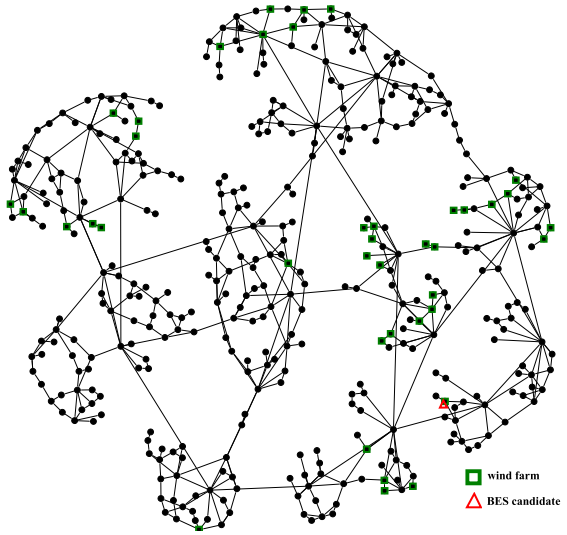

FIGURE 8. A provincial power grid of China employed as case study. The black circles are buses of 220 kV and over, the green squares are the wind farms and the red triangle denotes the candidate location of BESS.

Moreover, we compare the proposed method with the most frequently used scenario-based stochastic programming in Table.5, from the perspective of service life and total system cost during the entire cycle life of BESS. Here the

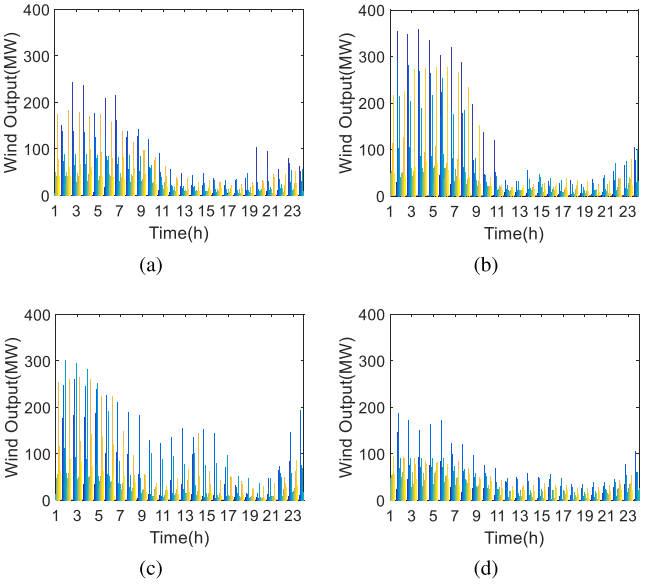

FIGURE 9. Typical output curves of wind farms in four seasons: (a) summer, (b) winter, (c) spring, and (d) autumn.

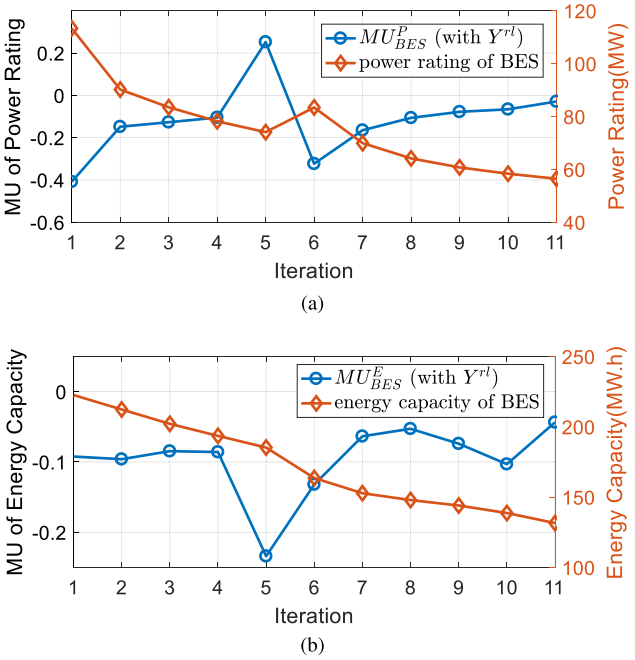

FIGURE 10. (a) Power rating reforming of BESS. (b) Energy capacity reforming of BESS.

operation cost includes generation cost and penalty on wind curtailment and load shedding. When applying SBSP to BESS sizing problem, there may be a big deviation between the expected life of BESS and the realistic one. Even if the anticipated life is accurate, such as 8 years in this case, the configuration plan derived through SBSP leads to higher system costs, since it fails to evaluate the revenue of BESS under hourly fluctuations of renewable generation during the whole life cycle.

TABLE 5. Cost of modified IEEE RTS-24 system with different BESS configurations (uniform annual value, unit: million USD per year).

Allocation Method	Results	Operation-dependent Evaluation			
		Realistic Life Y^{rl}	BES Investment Cost	Operation Cost	Total Cost
the Proposed Method	465.11MW.h,123.27MW	7.93	15.42566	511.4210	526.8467
SBSP ($Y^{\mathrm{ep}} = 6$)	479.4205MW.h,88.7324MW	7.98	15.48201	511.7722	527.2542
SBSP ($Y^{\mathrm{ep}} = 8$)	519.35MW.h,97.87MW	8.09	16.60748	510.4191	527.0265
SBSP ($Y^{\mathrm{ep}} = 10$)	622.8414MW.h,117.8086MW	8.23	19.63459	507.4805	527.1151

TABLE 6. Normalized typical daily total load profiles.

Time	Scen1	Scen2	Scen3	Scen4	Scen5	Scen6	Scen7	Scen8
1	0.813	0.470	0.546	0.452	0.559	0.452	0.547	0.350
2	0.780	0.469	0.541	0.416	0.541	0.447	0.536	0.338
3	0.750	0.457	0.539	0.394	0.527	0.446	0.521	0.340
4	0.726	0.450	0.531	0.384	0.515	0.439	0.509	0.338
5	0.702	0.445	0.529	0.384	0.506	0.438	0.506	0.335
6	0.682	0.453	0.541	0.401	0.523	0.447	0.517	0.332
7	0.689	0.484	0.585	0.419	0.548	0.484	0.558	0.361
8	0.689	0.478	0.639	0.454	0.545	0.481	0.543	0.379
9	0.714	0.475	0.702	0.452	0.534	0.452	0.546	0.365
10	0.779	0.497	0.750	0.425	0.563	0.457	0.582	0.376
11	0.845	0.520	0.773	0.411	0.595	0.459	0.611	0.388
12	0.922	0.543	0.796	0.428	0.629	0.471	0.639	0.411
13	0.963	0.534	0.782	0.414	0.624	0.464	0.642	0.417
14	0.972	0.523	0.772	0.378	0.623	0.457	0.640	0.401
15	0.953	0.525	0.763	0.377	0.629	0.462	0.639	0.394
16	0.933	0.531	0.760	0.379	0.640	0.463	0.649	0.396
17	0.909	0.542	0.768	0.398	0.648	0.464	0.655	0.408
18	0.888	0.555	0.811	0.452	0.655	0.490	0.662	0.440
19	0.866	0.556	0.826	0.503	0.644	0.504	0.655	0.474
20	0.864	0.558	0.819	0.510	0.640	0.513	0.661	0.464
21	0.915	0.572	0.792	0.511	0.653	0.507	0.659	0.448
22	0.945	0.566	0.732	0.492	0.648	0.495	0.650	0.427
23	0.928	0.551	0.658	0.451	0.620	0.479	0.625	0.397
24	0.862	0.513	0.590	0.405	0.573	0.449	0.582	0.361

C. VERIFICATION ON A PROVINCIAL SYSTEM OF CHINA

To demonstrate the scalability and efficiency of the proposed framework on practical size system, a provincial power system of China is adopted for case study, as shown in Fig.8. There are 398 buses of 220kV and over, 594 branches, 147 conventional generators and 82 wind farms in the system. Power flows through 220kV and over transmission lines are considered. Locations of wind farms are illustrated in Fig.8 with green square symbols. One centralized battery energy storage system is to be built with a connection point labeled by the red triangle symbol in Fig.8. We run yearly COS based on real load and wind power data of the grid from 2019.

We select 8 representative scenarios, which are working day of summer (Scen 1), non-working day of summer (Scen 2), working day of winter (Scen 3), non-working day of winter (Scen 4), working day of spring (Scen 5), non-working day of spring (Scen 6), working day of autumn (Scen 7) and non-working day of autumn (Scen 8). Normalized typical daily load profiles of the system are given in Table.6. The base value is selected as the maximum total power load of system in 2019, which is 6.4097×10^4MW. Typical curves of the 82 wind farms are illustrated in Fig.9.

The initial BES allocation plan is as follows: P^0_{BES} is 113.34.87MW and E^0_{BES} is 222.58.35MW.h, while the normalized marginal utility of this configuration is -40.86% and -9.23%, respectively. This indicates that the initial allocation through SBSP leads to an over investment on BESS, especially the power rating. After 11 rounds of iterations, the reformed BES size is: P^{11}_{BES} is 55.60MW, E^{11}_{BES} is 128.64MW.h with $MU^{\mathrm{P}}_{\mathrm{BES}}$ is -2.93%, $MU^{\mathrm{E}}_{\mathrm{BES}}$ is -4.36% and the realistic service life is $Y^{\mathrm{rl}} = 10.96$. The iterative size reforming process is shown in Fig.10.

VI. CONCLUSION

In this paper, we have proposed an optimal BESS sizing method considering the operation-dependent cycle life of batteries. It is showed that our two-level model can more accurately estimate the cycle-life deregulation of batteries and the revenue of BESS under hourly fluctuation of uncertain renewable generation, hence provides more reasonable sizing strategies. The tests on IEEE benchmark system and a real power grid demonstrate the effectiveness and practicality of the proposed method.

The scope of this work was limited to the sizing of battery energy storage in consideration of battery cycle-life. Installation location is not optimized. Therefore, it is recommended that future studies related to BESS allocation planning should consider the decision on installation location.

REFERENCES

[1] A. Sturt and G. Strbac, "Efficient stochastic scheduling for simulation of wind-integrated power systems," *IEEE Trans. Power Syst.*, vol. 27, no. 1, pp. 323–334, Feb. 2012.
[2] R. H. Byrne, T. A. Nguyen, D. A. Copp, B. R. Chalamala, and I. Gyuk, "Energy management and optimization methods for grid energy storage systems," *IEEE Access*, vol. 6, pp. 13231–13260, 2018.
[3] G. He, Q. Chen, C. Kang, P. Pinson, and Q. Xia, "Optimal bidding strategy of battery storage in power markets considering performance-based regulation and battery cycle life," *IEEE Trans. Smart Grid*, vol. 7, no. 5, pp. 2359–2367, Sep. 2016.
[4] P. Xiong and C. Singh, "Optimal planning of storage in power systems integrated with wind power generation," *IEEE Trans. Sustain. Energy*, vol. 7, no. 1, pp. 232–240, Jan. 2016.
[5] M. Asensio, P. Meneses de Quevedo, G. Munoz-Delgado, and J. Contreras, "Joint distribution network and renewable energy expansion planning considering demand response and energy storage—Part I: Stochastic programming model," *IEEE Trans. Smart Grid*, vol. 9, no. 2, pp. 655–666, Mar. 2018.

[6] M. Asensio, P. Meneses de Quevedo, G. Mu noz-Delgado, and J. Contreras, "Joint distribution network and renewable energy expansion planning considering demand response and energy storage—Part II: Numerical results," *IEEE Trans. Smart Grid*, vol. 9, no. 2, pp. 667–675, Mar. 2018.
[7] B. Odetayo, M. Kazemi, J. MacCormack, W. D. Rosehart, H. Zareipour, and A. Reza Seifi, "A chance constrained programming approach to the integrated planning of electric power generation, natural gas network and storage," *IEEE Trans. Power Syst.*, vol. 33, no. 6, pp. 6883–6893, Nov. 2018.
[8] R. A. Jabr, I. Dzafic, and B. C. Pal, "Robust optimization of storage investment on transmission networks," *IEEE Trans. Power Syst.*, vol. 30, no. 1, pp. 531–539, Jan. 2015.
[9] L. Yang, R. Xei, W. Wei, C. Sun, and S. Mei, "Coordinated planning of storage unit in a remote wind farm and grid connection line: A distributionally robust optimization approach," in *Proc. IEEE Innov. Smart Grid Technol. Asia (ISGT Asia)*, May 2019, pp. 424–428.
[10] I. J. Scott, P. M. S. Carvalho, A. Botterud, and C. A. Silva, "Clustering representative days for power systems generation expansion planning: Capturing the effects of variable renewables and energy storage," *Appl. Energy*, vol. 253, Nov. 2019, Art. no. 113603.
[11] R. Rao, S. Vrudhula, and D. N. Rakhmatov, "Battery modeling for energy-aware system design," *Computer*, vol. 36, no. 12, pp. 77–87, Dec. 2003.
[12] D. Tran and A. M. Khambadkone, "Energy management for lifetime extension of energy storage system in micro-grid applications," *IEEE Trans. Smart Grid*, vol. 4, no. 3, pp. 1289–1296, Sep. 2013.
[13] C. Liu, X. Wang, X. Wu, and J. Guo, "Economic scheduling model of microgrid considering the lifetime of batteries," *IET Gener., Transmiss. Distrib.*, vol. 11, no. 3, pp. 759–767, Feb. 2017.
[14] J.-O. Lee, Y.-S. Kim, T.-H. Kim, and S.-I. Moon, "Novel droop control of battery energy storage systems based on battery degradation cost in islanded DC microgrids," *IEEE Access*, vol. 8, pp. 119337–119345, 2020.
[15] X. Dong, Z. Yuying, and J. Tong, "Planning-operation co-optimization model of active distribution network with energy storage considering the lifetime of batteries," *IEEE Access*, vol. 6, pp. 59822–59832, 2018.
[16] S. D. Downing and D. F. Socie, "Simple rainflow counting algorithms," *Int. J. Fatigue*, vol. 1, no. 1, pp. 31–40, Jan. 1982.
[17] H. Abdeltawab and Y. A.-R.-I. Mohamed, "Mobile energy storage sizing and allocation for multi-services in power distribution systems," *IEEE Access*, vol. 7, pp. 176613–176623, 2019.
[18] Y. Liu, W. Du, L. Xiao, H. Wang, and S. Bu, "Sizing energy storage based on a life-cycle saving dispatch strategy to support frequency stability of an isolated system with wind farms," *IEEE Access*, vol. 7, pp. 166329–166336, 2019.
[19] Y. Zhang, Y. Xu, H. Yang, Z. Y. Dong, and R. Zhang, "Optimal whole-life-cycle planning of battery energy storage for multi-functional services in power systems," *IEEE Trans. Sustain. Energy*, vol. 11, no. 4, pp. 2077–2086, Oct. 2020.
[20] Z. Li, Q. Guo, H. Sun, and J. Wang, "Sufficient conditions for exact relaxation of complementarity constraints for storage-concerned economic dispatch," *IEEE Trans. Power Syst.*, vol. 31, no. 2, pp. 1653–1654, Mar. 2016.
[21] J. Fortuny-Amat and B. McCarl, "A representation and economic interpretation of a two-level programming problem," *J. Oper. Res. Soc.*, vol. 32, no. 9, pp. 783–792, Sep. 1981.
[22] P. Subcommittee, "IEEE reliability test system," *IEEE Trans. Power App. Syst.*, vols. PAS-98, no. 6, pp. 2047–2054, Nov. 1979.
[23] R. D. Zimmerman, C. E. Murillo-Sanchez, and R. J. Thomas, "MATPOWER: Steady-state operations, planning, and analysis tools for power systems research and education," *IEEE Trans. Power Syst.*, vol. 26, no. 1, pp. 12–19, Feb. 2011.
[24] P. Harsha and M. Dahleh, "Optimal management and sizing of energy storage under dynamic pricing for the efficient integration of renewable energy," *IEEE Trans. Power Syst.*, vol. 30, no. 3, pp. 1164–1181, May 2015.

YUNFAN ZHANG received the B.Sc. degree in electrical engineering from Tsinghua University, Beijing, China, in 2018, where she is currently pursuing the Ph.D. degree. Her research interests include applied optimization, energy economics, game theory, and their applications.

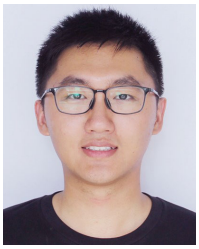

YIFAN SU received the B.Sc. degree in electrical engineering from Tsinghua University, Beijing, China, in 2019, where he is currently pursuing the Ph.D. degree. His research interests include distributed optimization and robust dispatch in smart grid.

ZHAOJIAN WANG (Member, IEEE) received the B.Sc. degree from Tianjin University, Tianjin, China, in 2013, and the Ph.D. degree from Tsinghua University, Beijing, China, in 2018. From 2016 to 2017, he was a Visiting Ph.D. Student at California Institute of Technology, CA, USA. From 2018 to 2020, he was a Postdoctoral Scholar with Tsinghua University. His research interests include power system stability analysis, distributed control, and microgrid planning.

FENG LIU (Senior Member, IEEE) received the B.Sc. and Ph.D. degrees in electrical engineering from Tsinghua University, Beijing, China, in 1999 and 2004, respectively. From 2015 to 2016, he was a Visiting Associate with the California Institute of Technology, CA, USA. He is currently an Associate Professor with Tsinghua University. He is the author or coauthor of more than 200 peer-reviewed technical articles and two books, and holds more than 20 issued or pending patents. His research interests include stability analysis, optimal control, robust dispatch, and game theory based decision making in energy and power systems. He is an Associate Editor of several international journals, including IEEE TRANSACTIONS ON SMART GRID and IEEE POWER AND ENERGY SOCIETY LETTER. He also served as a Guest Editor for IEEE TRANSACTIONS ON ENERGY CONVERSION.

CHENGHAO LI received the B.S. and Ph.D. degrees from the Huazhong University of Science and Technology, Wuhan, China, in 2009 and 2015, respectively. He is currently a Senior Engineer of State Grid Henan Electric Power Research Institute, China. His research interests include power systems, renewable energy integration, and energy storage systems.